Reliability Assessment of the Integrated Energy System Considering Gas–Thermal Inertia

Yaopei Zhu, Weijia Sun, Cairan Miao, Qi Wang*, Yi Tang and Yunkai Huang

School of Electrical Engineering, Southeast University, Nanjing, China

The electrical–thermal coupling integrated energy system (IES) has multi-timescale characteristics, and the gas–thermal slow dynamic characteristics of the IES contain rich flexibilities. The state of the gas–thermal system changes relatively with a time delay when the external conditions change, which can provide power support for the system over a certain timescale. Based on the gas–thermal inertia power support capability, a reliability assessment method of the IES considering gas–thermal inertia is proposed. According to research, the reliability assessment of the IES based on gas–thermal inertia can reduce the size and frequency of load shedding, alleviate the system operation risk caused by heavy load, reduce the system operation cost, and improve the system long-term operation reliability and economy. The greater the importance assessment index of energy conversion equipment, the greater its impact on system reliability, which is the weak node that should be focused on and protected.

Keywords: gas–thermal inertia, integrated energy system, load shedding, power support, reliability assessment

INTRODUCTION

An integrated energy system (IES) has the complementary characteristics of electricity, heat, and gas, which can promote the efficient utilization of energy and improve the absorption capacity of renewable energy (Pan et al., 2017; Fei et al., 2019). However, the multienergy coupling characteristics in the IES increase the operation complexity and uncertainty at the same time, which challenges the safe and reliable operation of the system (Mu et al., 2020; Wu et al., 2021). Therefore, it is necessary to fully exploit IES flexibility and ensure operation reliability and security through coordination and optimization (Wang et al., 2019). Compared with traditional power systems, the slow dynamic characteristics of gas–thermal system in the multienergy coupling IES contains rich flexibilities, which will help improve the reliability of system operation (Saldarriaga et al., 2013).

Regarding the slow dynamic characteristics of the thermal system, the concept of thermal inertia was mostly put forward in the research of the system optimization scheduling (Lei and Yi, 2018; Qin et al., 2019), flexibility assessment (Li et al., 2020a), and load recovery and frequency response strategies (Xu et al., 2019). Thermal inertia was considered as a response resource with scheduling value and verified to play a positive role in IES coordination operation. Only a few articles have conducted reliability assessment based on thermal inertia. For example, energy flow mutual reliability gain brought by thermal inertia was quantified (Li et al., 2020b), and inertia and transmission delay characteristics of the thermal network and modification of thermal supply reliability were considered. The above research only considered thermal inertia during the index calculation stage, and the reliability assessment index was modified accordingly. Thermal inertia did not actually participate in the calculation process of load shedding.

FIGURE 1 | Schematic diagram of gas and thermal inertia in the integrated energy system. **(A)** Scheme diagram of thermal inertia and **(B)** Scheme diagram of gas inertia.
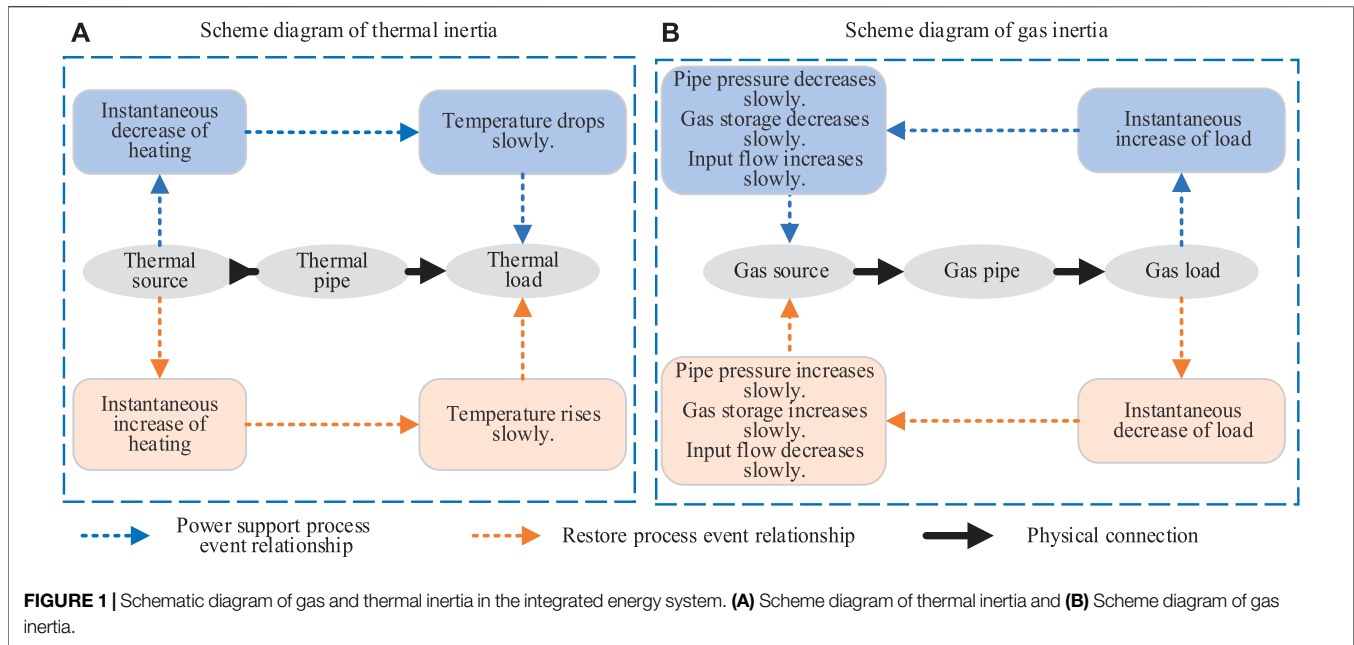
Regarding the slow dynamic characteristics of gas system, current studies mainly use the gas pipe storage characteristics to provide flexibility for IES optimal operation. The positive effects of gas pipe storage on improving IES flexibility were verified through the research on system optimization and scheduling (Fang et al., 2018; Liu et al., 2019; Bao et al., 2020), the mechanism of electrical interaction, flexibility assessment (Clegg and Mancarella, 2016), standby configuration (Antenucci and Sansavini, 2018), and optimal power flow calculation (Saedi et al., 2021). However, few studies have considered gas inertia in the reliability assessment of the IES.

To conclude, current studies mainly explore IES flexibility from the perspective of the gas pipe storage characteristics or thermal inertia characteristics of the thermal system, but few studies comprehensively consider both. At the same time, in terms of utilizing the flexibility of the gas–thermal system, the existing research mainly focused on how to coordinate and optimize the system but lacked basic mechanism analysis on how to consider the dynamic characteristics of the gas–thermal system in the reliability assessment of the IES. In fact, it is necessary to consider gas–thermal inertia in the reliability assessment of the IES when both gas storage and thermal inertia can provide power support for the system with buffer space.

Current innovation points generally lie in considering the influence of different factors on system reliability assessment when the research on IES reliability assessment is conducted. For example, considering the influence of multienergy storage (Cheng et al., 2020), comprehensive demand response, energy grade difference, and the operation strategy on system reliability, optimal load shedding is carried out in different scenarios, and the influence of different influencing factors on reliability assessment results is analyzed. In view of the problems existing in the current research, this study carries out a reliability assessment of the IES based on the characteristics of gas–thermal inertia to fully exploit the flexibility contained in the gas–thermal system and analyze the influence of gas–thermal inertia on the reliability of the IES. Therefore, this study, by considering the rich flexibility contained in the IES slow dynamic characteristics of the gas–thermal system, first establishes the reliability assessment model of the IES considering gas–thermal inertia, then analyzes the reliability assessment of specific processes, and finally analyzes the influence of gas–thermal inertia on the reliability assessment of the IES and studies the importance of different key equipment nodes for the long-term stable and reliable operation of the IES according to the rationality of the proposed model verified by actual examples.

ANALYSIS OF GAS–THERMAL INERTIA CHARACTERISTICS OF THE INTEGRATED ENERGY SYSTEM

Thermal energy in the IES has inertia characteristics, shown in **Figure 1A**. 1) Owing to the long transmission pipeline, there is a thermal delay of several minutes to several hours between the thermal source and the thermal load (Wei et al., 2022). 2) The thermal load can operate within the comfort zone and maintain a comfortable temperature for a long time owing to thermal inertia even if the thermal source is stopped. Therefore, the thermal load temperature changes relatively backward, and a comfortable temperature can be maintained in a certain period when the thermal source instantaneously changes owing to the thermal pipeline time delay and thermal load inertia.

In a similar manner, natural gas in the IES has inertial characteristics. As shown in **Figure 1B**, natural gas pipeline storage has negative feedback regulation characteristics

FIGURE 2 | Integrated energy system structure.
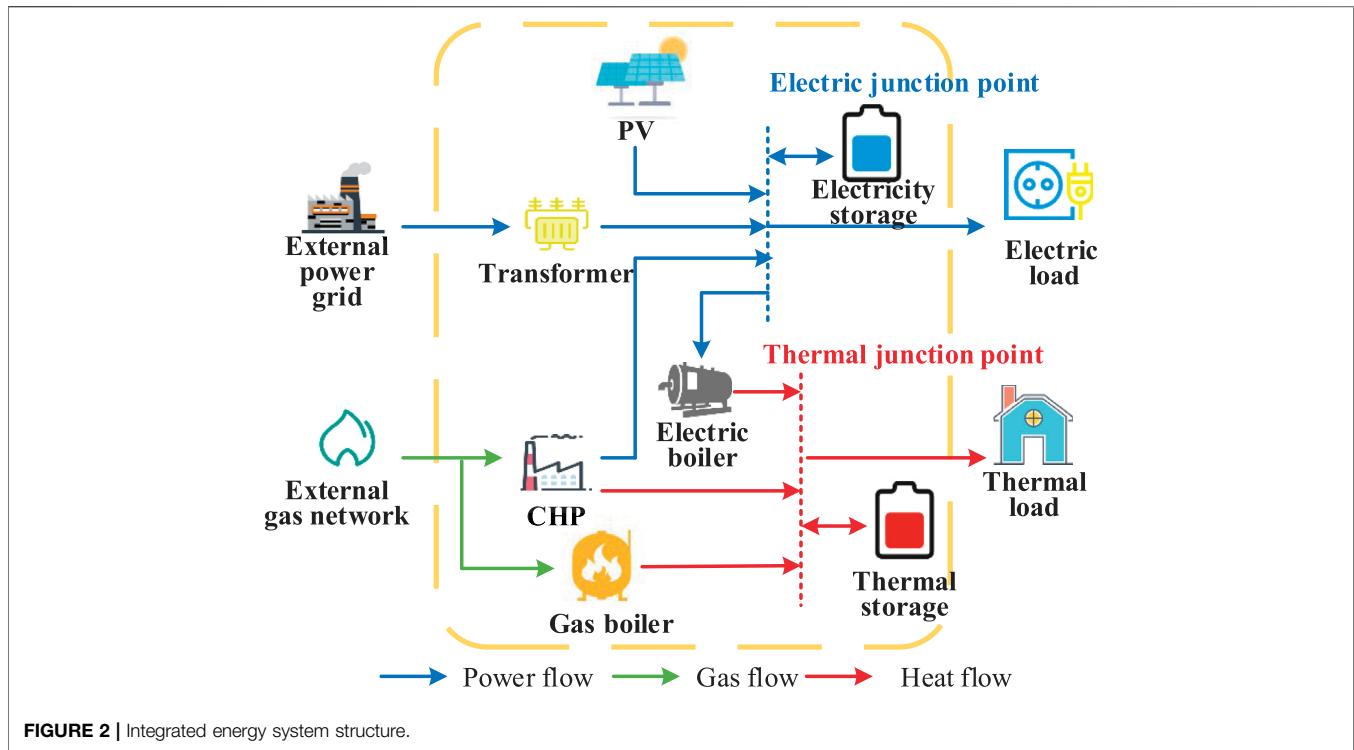
(Valdivia et al., 2020), which are as follows: 1) when the gas load increases, the transmission pipeline releases part of the pipe storage to the load, with the pipeline intensity of pressure and the pipe storage decreasing but the input flow increasing and 2) when the gas load decreases, the transmission pipeline stores the natural gas supplied by part of the gas source, with the pipeline intensity of pressure and the pipe storage increasing but the input flow decreasing. The specific principles are as follows: 1) When the gas load suddenly increases, the transmission pipe releases part of the pipe storage to the load in a short time, thereby allowing a large amount of gas to flow out of the pipe, which results in an increased flow rate. The amount of gas left at the pipe ends at that time will be less than before, thereby resulting in decreased pressure. 2) When the gas load suddenly decreases, the reduction of the load reduces the gas flow rate. Natural gas, that would otherwise be consumed, will accumulate in the pipeline, which increases the pipe pressure. Considering the similarity of principles, the intensity of pressure at the end of the gas pipeline is compared to the temperature of the thermal load, and the gas pipe storage is compared to the time delay and inertia of the thermal load. It can be concluded that the intensity of pressure at the end of the pipeline changes relatively backward owing to the existence of the gas pipe, and the appropriate intensity of pressure can be maintained within a certain period when load demand changes instantaneously.

To conclude, the system state changes relatively backward owing to the existence of buffer space and can maintain an acceptable state within a certain period. Therefore, gas–thermal inertia can provide external power support over a certain timescale.

RELIABILITY ASSESSMENT MODEL OF THE INTEGRATED ENERGY SYSTEM CONSIDERING GAS–THERMAL INERTIA

It is necessary to consider IES gas–thermal inertial power support capability when conducting the reliability assessment of the IES. Therefore, this section will establish the IES reliability assessment model considering the gas–thermal inertia.

System Structure
In this work, we study the IES structure shown in **Figure 2**. The system has two kinds of energy input: electric power and natural gas. The electric load is supplied by an external grid, a photovoltaic (PV), a combined heat and power (CHP) unit, and an electricity storage unit. The thermal load is supplied by an electric boiler, a CHP unit, a gas boiler, and a thermal storage unit. Components that may fail in the system include CHP units, electricity storage, an electric boiler, a gas boiler, and thermal storage.

Objective Function
The first condition aims at the least amount of the reduction of all types of loads. In the assessment cycle (this study takes 1 day as a complete scheduling cycle, which is equally divided into 24 periods), the maximum total energy supply and minimum load shedding of the system are regarded as the objective function. k represents the number of periods.

$$\max P^{\mathrm{L}} = \sum_{k=1}^{24} \left(P_k^{\mathrm{EL}} + P_k^{\mathrm{HL}} \right) \tag{1}$$

P^L is the total energy supply of the IES. P_k^{EL} is the total energy supply of the IES in time k. P_k^{HL} is the total thermal energy of the IES in time k.

$$\min P^{\mathrm{LC}} = \sum_{k=1}^{24} \left[\left(P_k^{\mathrm{ELf}} - P_k^{\mathrm{EL}} \right) + \left(P_k^{\mathrm{HLf}} - P_k^{\mathrm{HL}} \right) \right] \tag{2}$$

P^{LC} is the total amount of load shedding. P_k^{Elf} is the forecasting output of electric load in the IES in time k. P_k^{HLf} is the forecasting output of thermal load in the IES in time k.

The second condition includes the cost of compensation for load shedding and the cost of gas–thermal inertia output in the total cost and aims at minimum operating cost. In the assessment cycle, the minimum system operating cost is regarded as the objective function.

$$\begin{aligned}
\min C &= C^{\mathrm{E}} + C^{\mathrm{G}} + C^{\mathrm{GR}} + C^{\mathrm{HR}} + C^{\mathrm{EC}} + C^{\mathrm{HC}} \\
&= \sum_{k=1}^{24} \left[c_k^{\mathrm{E}} \cdot P_k^{\mathrm{E}} + c^{\mathrm{G}} \cdot P_k^{\mathrm{G}} + c^{\mathrm{GR}} \cdot R_k^{\mathrm{G}} + c^{\mathrm{HR}} \cdot R_k^{\mathrm{H}} \right. \\
&\left. + c^{\mathrm{EC}} \cdot \left(P_k^{\mathrm{ELf}} - P_k^{\mathrm{EL}} \right) + c^{\mathrm{HC}} \cdot \left(P_k^{\mathrm{HLf}} - P_k^{\mathrm{HL}} \right) \right]
\end{aligned} \tag{3}$$

C is the total cost of the IES. C^E is the output cost of the electrical power grid. C^G is the output cost of the gas network. C^{GR} is the output cost of gas inertia. C^{HR} is the output cost of thermal inertia. C^{EC} is the electric load shedding compensation cost. C^{HC} is the thermal load shedding compensation cost. c_k^E is the unit output cost of the electrical power grid. c^G is the unit output cost of the gas network. c^{GR} is the unit output cost of gas inertia. c^{HR} is the unit output cost of thermal inertia. c^{EC} is the electric load shedding compensation unit cost. c^{HC} is the thermal load shedding compensation unit cost.

Constraint Conditions

According to the actual operation of the IES, the constraints are described as follows.

1) Electrical and thermal power balance

The electrical power balance is as follows:

$$P_k^{\mathrm{PVf}} + \eta^{\mathrm{T}} f_k^{\mathrm{E}} P_k^{\mathrm{E}} + f_k^{\mathrm{CHP}} P_k^{\mathrm{CHP,e}} + f_k^{\mathrm{ES,discharge}} P_k^{\mathrm{ES,discharge}} + R_k^{\mathrm{G}}$$
$$= P_k^{\mathrm{EL}} + f_k^{\mathrm{EB}} P_k^{\mathrm{EB,e}} + f_k^{\mathrm{ES,charge}} P_k^{\mathrm{ES,charge}} \tag{4}$$

$$P_k^{\mathrm{EL}} \leq P_k^{\mathrm{ELf}} \tag{5}$$

P_k^{PVf} is the PV forecast output in time k. η^T is the transformer operating efficiency. P_k^E is the external power grid energy supply in time k. $P_k^{CHP,e}$ is the CHP unit power supply in time k. $P_k^{ES,discharge}$ is the energy released by electricity storage in time k. P_k^{EL} is the actual electric load supplied by the IES in time k. P_k^{Elf} is the electric load forecast output in time k. $P_k^{EB,e}$ is the electrical energy supplied into the electric boiler in time k. $P_k^{ES,charge}$ is the energy supplied into electricity storage in time k. f_k^E is the state of energy supply of the external power grid. f_k^{CHP} is the working state of CHP units. $f_k^{ES,discharge}$ is the energy discharging state of electricity storage. f_k^{EB} is the working state of the electric boiler. $f_k^{ES,charge}$ is the energy charging state of electricity storage. f_k^{EB} is the working state of the electric boiler.

The thermal power balance is as follows:

$$f_k^{\mathrm{EB}} P_k^{\mathrm{EB,h}} + f_k^{\mathrm{CHP}} P_k^{\mathrm{CHP,h}} + f_k^{\mathrm{GB}} P_k^{\mathrm{GB,h}} + f_k^{\mathrm{HS,discharge}} P_k^{\mathrm{HS,discharge}}$$
$$= P_k^{\mathrm{HL}} - R_k^{\mathrm{H}} + f_k^{\mathrm{HS,charge}} P_k^{\mathrm{HS,charge}} \tag{6}$$

$$P_k^{\mathrm{HL}} \leq P_k^{\mathrm{HLf}} \tag{7}$$

$P_k^{EB,h}$ is the thermal energy output from the electric boiler in time k. $P_k^{CHP,h}$ is the thermal energy output from CHP units in time k. $P_k^{GB,h}$ is the thermal energy output from the gas boiler in time k. $P_k^{HS,discharge}$ is the energy discharged by thermal storage in time k. P_k^{HL} is the actual thermal load supplied by the IES in time k. P_k^{HLf} is the forecast thermal load output in time k. $P_k^{HS,charge}$ is the energy charged in thermal storage in time k. R_k^H is the power support provided by thermal inertia in time k. f_k^{GB} is the working state of the gas boiler. $f_k^{HS,discharge}$ is the energy discharged state of thermal storage. $f_k^{HS,charge}$ is the energy charged state of thermal storage.

2) Energy supply–side constraint

Power supply constraints are as follows:

$$\begin{cases} P_{\min}^{\mathrm{E}} \leq P_k^{\mathrm{E}} \leq P_{\max}^{\mathrm{E}} \\ -P_{\mathrm{down}}^{\mathrm{S}} \Delta k \leq P_k^{\mathrm{E}} - P_{k-1}^{\mathrm{E}} \leq P_{\mathrm{up}}^{\mathrm{S}} \Delta k \end{cases} \tag{8}$$

P_{min}^E is the minimum input for the external power grid. P_{max}^E is the maximum input for the external power grid. P_{up}^S is the upper climbing rate limits for the external power grid input. P_{down}^S is the lower climbing rate limits for the external power grid input. $\triangle k$ is the k period.

Gas supply constraints are as follows:

$$\begin{cases} P_{\min}^{\mathrm{G}} \leq P_k^{\mathrm{G}} \leq P_{\max}^{\mathrm{G}} \\ -P_{\mathrm{down}}^{\mathrm{G}} \Delta k \leq P_k^{\mathrm{G}} - P_{k-1}^{\mathrm{G}} \leq P_{\mathrm{up}}^{\mathrm{G}} \Delta k \end{cases} \tag{9}$$

P_{min}^G is the minimum input for the external gas network. P_{max}^G is the maximum input for the external gas network. P_{up}^G is the upper climbing rate limits for the external gas network input. P_{down}^G is the lower climbing rate limits for the external gas network input. P_k^G is the power supply from the external power grid in time k.

3) Energy conversion and energy storage–side constraints

CHP unit constraints are as follows:

$$\begin{cases} P_k^{\mathrm{G}} + R_k^{\mathrm{G}} = P_k^{\mathrm{CHP}} + P_k^{\mathrm{GB}} \\ P_k^{\mathrm{CHP,e}} = \eta_{\mathrm{ge}}^{\mathrm{CHP}} P_k^{\mathrm{CHP}} \\ P_k^{\mathrm{CHP,h}} = \eta_{\mathrm{gh}}^{\mathrm{CHP}} P_k^{\mathrm{CHP}} \\ P_{\min}^{\mathrm{CHP}} \leq P_k^{\mathrm{CHP}} \leq P_{\max}^{\mathrm{CHP}} \\ -P_{\mathrm{down}}^{\mathrm{CHP}} \Delta k \leq P_k^{\mathrm{CHP}} - P_{k-1}^{\mathrm{CHP}} \leq P_{\mathrm{up}}^{\mathrm{CHP}} \Delta k \end{cases} \tag{10}$$

R_k^G is the power support provided by gas inertia in time k. P_k^{CHP} is the input power to CHP units in time k. P_k^{GB} is the input power to the gas boiler units in time k. η_{ge}^{CHP} is the efficiency of CHP units to generate electrical energy. η_{ge}^{CHP} is the efficiency of CHP units to generate thermal energy. P_{max}^{CHP} is the upper limit of CHP unit input power. P_{min}^{CHP} is the lower limit of CHP unit input power. P_{up}^{CHP} is the upper limit of the climbing rate of CHP

unit input power. $P_{down}{}^{CHP}$ is the lower limit of the climbing rate of CHP unit input power. $\triangle k$ is the k time period.

Electric boiler constraints are as follows:

$$\begin{cases} P_k^{\mathrm{EB,h}} = \eta^{\mathrm{EB}} P_k^{\mathrm{EB,e}} \\ P_{\min}^{\mathrm{EB}} \leq P_k^{\mathrm{EB,e}} \leq P_{\max}^{\mathrm{EB}} \\ -P_{\mathrm{down}}^{\mathrm{EB}} \Delta k \leq P_k^{\mathrm{EB,e}} - P_k^{\mathrm{EB,e}} \leq P_{\mathrm{up}}^{\mathrm{EB}} \Delta k \end{cases} \tag{11}$$

η^{EB} is the efficiency of the electric boiler. $P_{min}{}^{EB}$ is the lower limit of the electric boiler input power. $P_{max}{}^{EB}$ is the upper limit of the electric boiler input power. $P_{up}{}^{EB}$ is the upper limit of the climbing rate of the electric boiler input power. $P_{down}{}^{EB}$ is the lower limit of the climbing rate of the electric boiler input power. $\triangle k$ is the k time period.

Gas boiler constraints are as follows:

$$\begin{cases} P_k^{\mathrm{GB,h}} = \eta^{\mathrm{GB}} P_k^{\mathrm{GB}} \\ P_{\min}^{\mathrm{GB}} \leq P_k^{\mathrm{GB}} \leq P_{\max}^{\mathrm{GB}} \\ -P_{\mathrm{down}}^{\mathrm{GB}} \Delta k \leq P_k^{\mathrm{GB}} - P_k^{\mathrm{GB}} \leq P_{\mathrm{up}}^{\mathrm{GB}} \Delta k \end{cases} \tag{12}$$

η^{GB} is the efficiency of the gas boiler. $P_{min}{}^{GB}$ is the lower limit of the gas boiler input power. $P_{max}{}^{GB}$ is the upper limit of the gas boiler input power. $P_{up}{}^{GB}$ is the upper limit of the climbing rate of the gas boiler input power. $P_{down}{}^{GB}$ is the lower limit of the climbing rate of the gas boiler input power. $\triangle k$ is the k time period.

Electricity storage constraints are as follows:

$$\begin{cases} f_k^{\mathrm{ES,discharge}} + f_k^{\mathrm{ES,charge}} \leq 1 \\ f_k^{\mathrm{ES,discharge}} P_{\min}^{\mathrm{ES,discharge}} \leq P_k^{\mathrm{ES,discharge}} \leq f_k^{\mathrm{ES,discharge}} P_{\max}^{\mathrm{ES,discharge}} \\ f_k^{\mathrm{ES,charge}} P_{\min}^{\mathrm{ES,charge}} \leq P_k^{\mathrm{ES,charge}} \leq f_k^{\mathrm{ES,charge}} P_{\max}^{\mathrm{ES,charge}} \\ C_{k+1}^{\mathrm{ES}} = C_k^{\mathrm{ES}}(1 - \delta_{\mathrm{ES}}) + \left(P_k^{\mathrm{ES,charge}} \eta^{\mathrm{ES,charge}} - P_k^{\mathrm{ES,discharge}} / \eta^{\mathrm{ES,discharge}} \right) \Delta k \\ C_{\min}^{\mathrm{ES}} \leq C_k^{\mathrm{ES}} \leq C_{\max}^{\mathrm{ES}} \end{cases} \tag{13}$$

$P_{max}{}^{ES,discharge}$ is the upper limit of electricity storage discharging power. $P_{min}{}^{ES,discharge}$ is the lower limit of electricity storage discharging power. $P_{max}{}^{ES,charge}$ is the upper limit of electricity storage charging power. $P_{min}{}^{ES,charge}$ is the lower limit of electricity storage charging power. $C_k{}^{ES}$ is the capacity of electricity storage. δ_{ES} is the energy loss rate of electricity storage. $\eta_{ES}^{discharge}$ is the discharging efficiency of electricity storage. η_E^{charge} is the charging efficiency of electricity storage. $C_{min}{}^{ES}$ is the lower limit of electricity storage capacity. $C_{max}{}^{ES}$ is the upper limit of electricity storage capacity. $\triangle k$ is the k time period.

Thermal storage constraints are as follows:

$$\begin{cases} f_k^{\mathrm{HS,discharge}} + f_k^{\mathrm{HS,charge}} \leq 1 \\ f_k^{\mathrm{HS,discharge}} P_{\min}^{\mathrm{HS,discharge}} \leq P_k^{\mathrm{HS,discharge}} \leq f_k^{\mathrm{HS,discharge}} P_{\max}^{\mathrm{HS,discharge}} \\ f_k^{\mathrm{HS,charge}} P_{\min}^{\mathrm{HS,charge}} \leq P_k^{\mathrm{HS,charge}} \leq f_k^{\mathrm{HS,charge}} P_{\max}^{\mathrm{HS,charge}} \\ C_{k+1}^{\mathrm{HS}} = C_k^{\mathrm{HS}}(1 - \delta_{\mathrm{HS}}) + \left(P_k^{\mathrm{HS,charge}} \eta^{\mathrm{HS,charge}} - P_k^{\mathrm{HS,discharge}} / \eta^{\mathrm{HS,discharge}} \right) \Delta k \\ C_{\min}^{\mathrm{HS}} \leq C_k^{\mathrm{HS}} \leq C_{\max}^{\mathrm{HS}} \end{cases} \tag{14}$$

$P_{min}{}^{HS,discharge}$ is the lower limit of heat storage discharging power. $P_{max}{}^{HS,discharge}$ is the upper limit of heat storage discharging power. $P_{min}{}^{HS,charge}$ is the lower limit of heat storage charging power. $P_{max}{}^{HS,charge}$ is the upper limit of heat

storage charging power. $C_k{}^{HS}$ is the capacity of heat storage. δ_{HS} is the energy loss rate of heat storage. η_{HS}^{Charge} is the charging efficiency of heat storage. $\eta_{HS}^{discharge}$ is the discharging efficiency of heat storage. $C_{min}{}^{HS}$ is the lower limit of heat storage capacity. $C_{max}{}^{HS}$ is the upper limit of heat storage capacity.

4) Gas–thermal inertia constraints

Gas inertia constraints are as follows:

$$\begin{cases} 0 \leq R_k^{\mathrm{G}} \leq S_k^{\mathrm{G}} R_{\max}^{\mathrm{G}} \\ 0 \leq o_k^{\mathrm{G}} \leq \max\_ON^{\mathrm{G}} \\ f_{k+o_k^{\mathrm{G}}}^{\mathrm{G}} \geq \min\_OFF^{\mathrm{G}} \end{cases} \tag{15}$$

S_k^G is the 0–1 variable. $S_k^G = 1$ means that gas inertia is used. $S_k^G = 0$ means that gas inertia is not used. $R_{max}{}^G$ is the maximum value of gas inertia that can be used. The specific time is that the maximum gas standby time in every 6 h is set to be no more than 3 h. $o_k{}^G$ is the continuous running time of the gas inertia reserve in time k. max_ON^G is the longest continuous running time of the gas inertia reserve. f_{k+} $o_k{}^{G}$ ^{G} is the time interval of the gas inertia reserve in period $(k + o_k{}^G)$. min_OFF^G is the minimum interval of the gas inertia reserve.

Thermal inertia constraints are as follows:

$$\begin{cases} 0 \leq R_k^{\mathrm{H}} \leq S_k^{\mathrm{H}} R_{\max}^{\mathrm{H}} \\ 0 \leq o_k^{\mathrm{H}} \leq \max\_ON^{\mathrm{H}} \\ f_{k+o_k^{\mathrm{H}}}^{\mathrm{H}} \geq \min\_OFF^{\mathrm{H}} \end{cases} \tag{16}$$

S_k^H is the 0–1 variable. $S_k^H = 1$ means that thermal inertia is used. $S_k^H = 0$ means that thermal inertia is not used. $R_{max}{}^H$ is the maximum value of thermal inertia that can be used. The specific time is the maximum thermal standby time in every 10 h that is set to be no more than 5 h. $o_k{}^H$ is the continuous running time of the thermal inertia reserve in time k. max_ON^H is the longest continuous running time of the thermal inertia reserve. f_{k+} $o_k{}^{H}$ is the time interval of the thermal inertia reserve in the period $(k + o_k{}^H)$. min_OFF^H is the minimum interval of the thermal inertia reserve.

4) Integrated energy system reliability assessment process considering gas–thermal inertia

The steps of IES reliability assessment considering gas–thermal inertia, shown in **Figure 3**, mainly include four parts: load and PV annual data generation, component annual state generation, optimal load shedding optimization, and reliability assessment index calculation (Bansal et al., 2014).

Load and Photovoltaic Annual Data Generation

Divide a year into 8,760 periods, each of which is 1 h. The required data for electric load, thermal load, and PV year per hour are captured as follows from the actual historical data of the IES (sampling once every 15 min), and the results will be used as data input parameters.
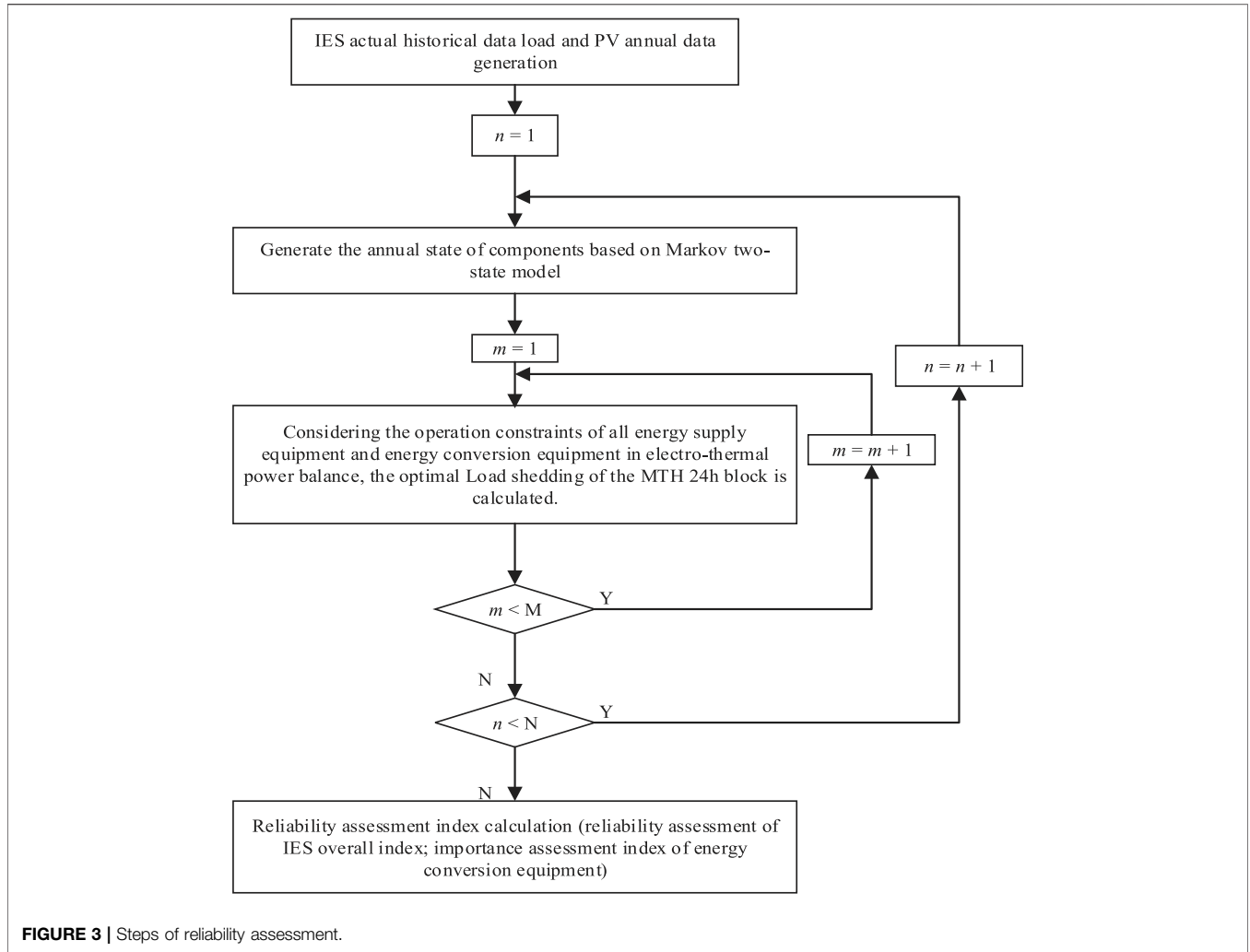
FIGURE 3 | Steps of reliability assessment.

$$\begin{cases} P_k^{\text{ELf}} = p_{4k}^{\text{EL}} \\ P_k^{\text{HLf}} = p_{4k}^{\text{HL}} \\ P_k^{\text{PVf}} = p_{4k}^{\text{PV}} \end{cases} \tag{17}$$

$P_{4k}{}^{EL}$ is the electrical load power of the IES at sampling point $4k$. $P_{4k}{}^{HL}$ is the thermal load power of the IES at sampling point $4k$. $P_{4k}{}^{PVf}$ is the PV output of IES at sampling point $4k$.

Component Year State Generation

Based on the Markov two-state model, the annual state of components is generated, and the Monte Carlo method is used to simulate the state change behavior of IES components within 1 year. The results will be used as input parameters of availability state variables.

The component i shutdown model is obtained as follows (Wei et al., 2020):

$$p^i(t) = 1 - e^{-\mu t} \tag{18}$$

i is the component and μ is the component repair rate.

The random number $R_{d.\ t}{}^i$ is generated in the evenly distributed [0,1]:

$$f_{d,t}^i = \begin{cases} 0, R_{d,t}^i > p^i(t)\,(\text{working state}) \\ 1, R_{d,t}^i \le p^i(t)\,(\text{shutdown state}) \end{cases} \tag{19}$$

$f_{d.t}{}^i$ is the equipment state of component i in time t at the αth day. $R_{d.\ t}{}^i$ is the random number.

The overall state of the system components can be obtained as follows:

$$p^i(t) = \left(f_t^{\text{CHP}}, f_t^{\text{GB}}, f_t^{\text{EB}}, f_t^{\text{ES,charge}}, f_t^{\text{HS,charge}} \right) \tag{20}$$

Optimal Load Shedding Optimization

The specific steps of optimal load shedding optimization are as follows:

Step 1: Set the initial value of Monte Carlo random simulation times $n = 1$ and the total random simulation times $N = 1,000$.

Step 2: Set the initial value of the annual optimal load shedding calculation block $m = 1$ and the total number of random simulations $M = 365$.

Step 3: Select the mth 24-h block and calculate the optimal load shedding with 24 h as the whole cycle based on the generated source

TABLE 1 | Descriptions of different cases.

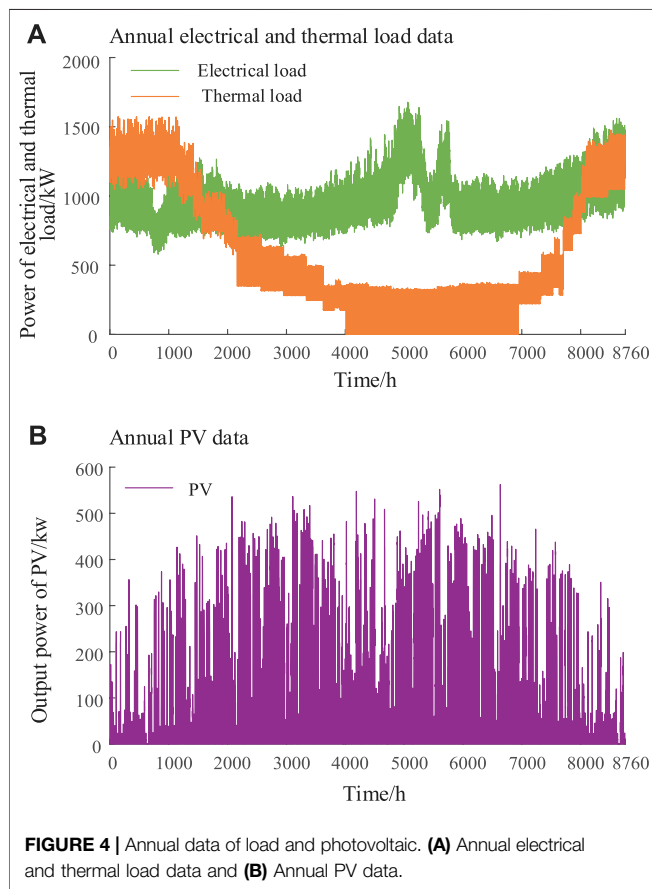| Case	Description
Case 1 to Case 7	Considering gas–thermal inertia and aiming at the minimum load shedding, the reliability assessment of the IES is carried out. It is assumed that all equipment is in normal operation or only the failure of/electric boiler/gas boiler/electricity storage/thermal storage is considered or all equipment may fail.
Case 8 to Case 14	Considering the gas–thermal inertia and aiming at the minimum operating cost, the reliability assessment of the IES is carried out. It is assumed that all equipment is in normal operation or only the failure of CHP units/electric boiler/gas boiler/electricity storage/thermal storage is considered or all equipment may fail.
Case 15 to Case 21	In the absence of gas–thermal inertia, the reliability assessment of the IES is carried out with the goal of minimizing the load shedding. It is assumed that all equipment is in normal operation or only the failure of CHP unit/electric boiler/gas boiler/electricity storage/thermal storage is considered or all equipment may fail.
Case 22 to Case 28	Without the consideration of gas–thermal inertia, the reliability assessment of the IES is carried out with the goal of minimizing operating cost. It is assumed that all equipment is in normal operation or only failure of CHP unit/electric boiler/gas boiler/electricity storage/thermal storage is considered or all equipment may fail.

FIGURE 4 | Annual data of load and photovoltaic. **(A)** Annual electrical and thermal load data and **(B)** Annual PV data.

TABLE 3 | Comparison results of Case 7 and Case 21.

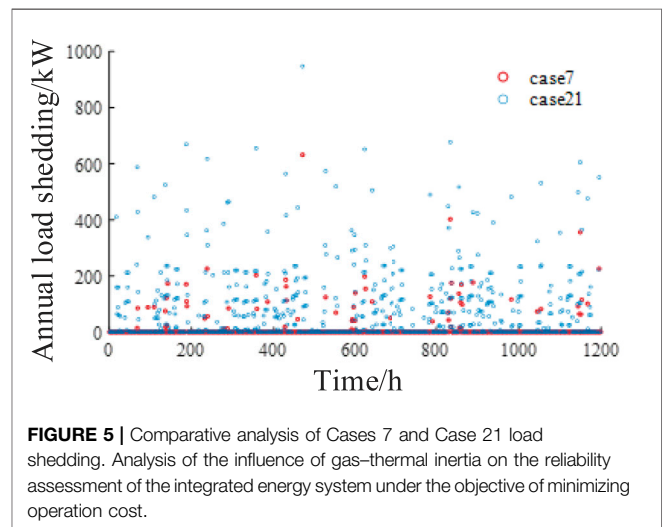| Assessment indicators	Case 7	Case 21
Annual maximum energy supply/kW	13,277,475	13,268,976
Annual maximum electricity supply/kW	8,694,851	8,691,089
Annual maximum thermal capacity/kW	4,613,436	4,577,887
Annual total load shedding/kW	77,049	85,548
Annual total load shedding/kW	46,238	50,000
Annual total cutting thermal load/kW	30,811	35,548
Annual energy shortage time/h	137	564
Annual energy shortage probability	1.56%	6.44%

FIGURE 5 | Comparative analysis of Cases 7 and Case 21 load shedding. Analysis of the influence of gas–thermal inertia on the reliability assessment of the integrated energy system under the objective of minimizing operation cost.

TABLE 2 | Failure rate of each key equipment node.

Device node	Failure rate
Cogeneration unit	0.01548493
Electric boiler	0.01100000
Gas boiler	0.00547945
Electronic storage	0.00014000
Thermal storage	0.00014000

load data and element state while comprehensively considering the electrical and thermal power balance and the operation constraints of each energy supply device and energy conversion device.

Step 4: If $m = 365$, the annual optimal load shedding process ends, and the process moves to step 5. If $m < 365$, go to step 3, where $m = m + 1$.

Step 5: If $n = 1,000$, the Monte Carlo random simulation process ends. If $n < 1,000$, go to step 2, where $n = n + 1$.

TABLE 4 | Comparison results of Case 14 and Case 28.

Assessment indicators	Case14	Case28
Annual operating cost/¥	8,121,013	11,602,724
Annual maximum energy supply/kW	13,293,738	13,218,052
Annual maximum electricity supply/kW	8,697,063	8,648,843
Annual maximum thermal capacity/kW	4,596,676	4,569,210
Annual total load shedding/kW	60,786	136,472
Annual total load shedding/kW	44,026	92,246
Annual total cutting thermal load/kW	16,760	44,226
Annual energy shortage time/h	148	616
Annual energy shortage probability	1.69%	7.03%
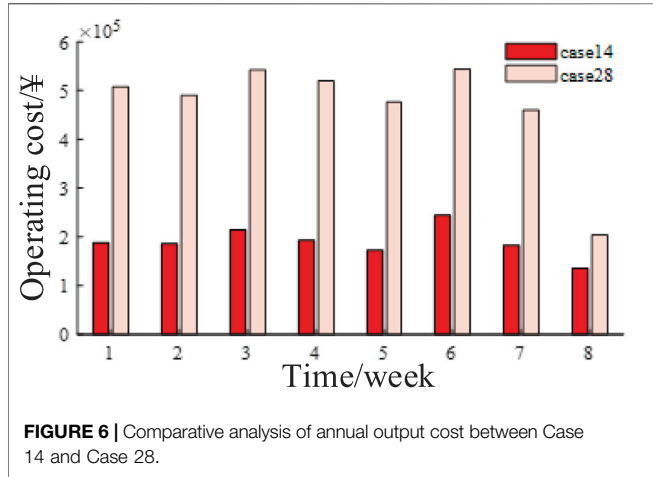
FIGURE 6 | Comparative analysis of annual output cost between Case 14 and Case 28.

Calculation of Reliability Assessment Index

The overall index of IES reliability assessment can be obtained by averaging the optimal load shedding optimization under multiple Monte Carlo random simulations, in which $P_{ave}{}^{LC}$, $P_{ave}{}^{ELC}$, and $P_{ave}{}^{HLC}$ can be expressed as follows:

$$\begin{cases} P_{ave}^{LC} = \dfrac{\sum\limits_{n=1}^{N}\sum\limits_{m=1}^{M}\sum\limits_{k=1}^{24}\left[\left(P_k^{ELf} - P_k^{EL}\right) + \left(P_k^{HLf} - P_k^{HL}\right)\right]}{N} \\[2mm] P_{ave}^{ELC} = \dfrac{\sum\limits_{n=1}^{N}\sum\limits_{m=1}^{M}\sum\limits_{k=1}^{24}\left[\left(P_k^{ELf} - P_k^{EL}\right)\right]}{N} \\[2mm] P_{ave}^{HLC} = \dfrac{\sum\limits_{n=1}^{N}\sum\limits_{m=1}^{M}\sum\limits_{k=1}^{24}\left[\left(P_k^{HLf} - P_k^{HL}\right)\right]}{N} \end{cases} \quad (21)$$

$P_{ave}{}^{LC}$ is the annual total load shedding amount. $P_{ave}{}^{ELC}$ is the total annual electrical power load shedding. $P_{ave}{}^{HLC}$ is the total annual thermal load shedding.

Annual energy shortage time $t_{ave}{}^{C}$ and annual energy shortage probability $p_{ave}{}^{C}$ can be expressed as follows:

$$\begin{cases} t_{ave}^{C} = \dfrac{\sum\limits_{n=1}^{N} t_n^{C}}{N} \\[2mm] p_{ave}^{C} = \dfrac{t_{ave}^{C}}{8760} \end{cases} \quad (22)$$

$t_{ave}{}^{C}$ is the annual energy shortage time. $p_{ave}{}^{C}$ is the annual energy shortage probability. $t_n{}^{C}$ is the number of hours with insufficient energy in the year in the nth Monte Carlo random simulation.

The importance assessment index s^i of the energy conversion equipment i is expressed as follows: the larger the importance assessment index, the greater the influence of the energy conversion equipment on the system's reliability.

$$s^i = \frac{P_{ave}^{LC,i}}{P_{ave}^{LC}} \quad (23)$$

s^i is the importance assessment index. $P_{ave}{}^{LC,i}$ is the annual total load shedding when only the energy conversion device i fails.

CASE STUDY

In this article, the YALMIP toolbox is run in MATLAB 2020a, and Gurobi9.1.1 is used to solve the above mixed integer linear programming problem. To verify the influence of gas–thermal inertia on reliability assessment results of the IES and analyze the importance of different key equipment nodes for the long-term stable and reliable operation of the IES, various cases are considered for comparative analysis, as shown in **Table 1**.
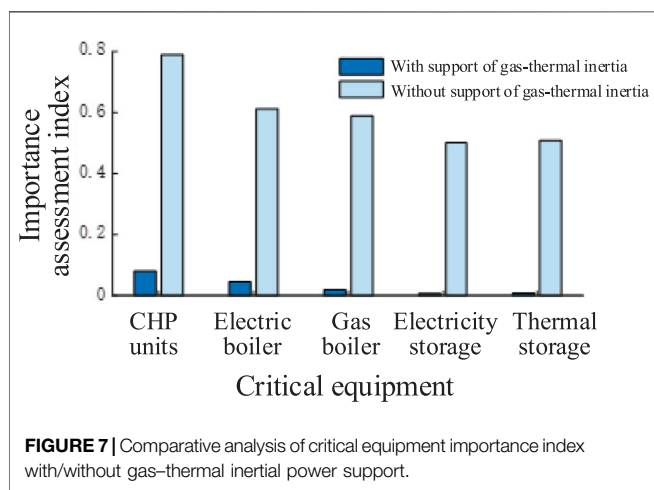
The annual data of electrical and thermal loads and PV in the actual IES are shown in **Figures 4A,B**, respectively, and the failure rate of each key equipment node is shown in **Table 2**.

Analysis of Influence of Gas–Thermal Inertia on the Reliability Assessment of an Integrated Energy System with Minimum Load Shedding

A 1-year long-term reliability assessment is carried out considering the minimum load shedding as the goal and

TABLE 5 | Results of Case 2 to Case 6.

Case	Annual total load shedding/kW	Key equipment	Importance assessment index
Case 2	6,271	Cogeneration unit	0.0814
Case 3	3,572	Electric boiler	0.0464
Case 4	1,484	Gas boiler	0.0193
Case 5	559	Electronic storage	0.0073
Case 6	615	Thermal storage	0.0080

According to the above results, the order of importance of each key equipment is as follows: CHP unit > electric boiler > gas boiler > thermal storage > electricity storage.

TABLE 6 | Results of Case 16 to Case 20.

Case	Annual total load shedding/kW	Key equipment	Importance assessment index
Case 16	67,515	Cogeneration unit	0.7892
Case 17	52,410	The electric boiler	0.6126
Case 18	50,430	Gas boiler	0.5895
Case 19	43,008	Electronic storage	0.5027
Case 20	43,567	Thermal storage	0.5093

FIGURE 7 | Comparative analysis of critical equipment importance index with/without gas–thermal inertial power support.

including/excluding the gas–thermal inertia of the IES. The comparison results are shown in **Table 3**. Considering gas–thermal inertia, the power support effectively reduces the annual total load shedding of the system and increases the maximum total energy supply, in which the maximum electricity and thermal supplies increase, while the annual energy shortage time and energy shortage probability decrease obviously.

The annual load shedding data in the scenario are shown in **Figure 5**, when the annual state of typical components is selected and gas–thermal inertia is included/excluded. In a year, when the total electrical and thermal loads are high, the event of insufficient energy supply is more likely to occur. Compared with Case 21 without gas–thermal inertia power support, Case 7 with gas–thermal inertia included significantly reduces the number of load shedding actions, and the load shedding amplitude decreases to a certain extent. It can be known that considering the power support effect of the gas–thermal inertia of the IES, the size and frequency of load shedding can be reduced simultaneously, the system operation risk caused by heavy load can be effectively alleviated, and the long-term operation reliability of the system can be improved.

A 1-year long-term reliability assessment is carried out with the goal of minimizing the operating cost and including/ excluding the gas–thermal inertia of the IES. The results are shown in **Table 4**. Considering the power support of gas–thermal inertia, the annual operating cost of the system is significantly reduced, and the economy is optimized. At the same time, the

maximum energy supply of the system is increased, the amplitude, time, and frequency of load shedding are reduced correspondingly, and the reliability of the IES is obviously improved.

The annual load shedding data in the scenario are shown in **Figure 6**, when the annual state of typical components is selected and gas–thermal inertia is included/excluded (in order to highlight the difference between Case 28 and Case 14, the data of the first 2 months with higher total electrical and thermal loads are selected for comparison).

Compared with that of Case 28 without gas–thermal inertia power support, the operating cost of Case 14 with gas–thermal inertia is significantly reduced due to the reduction in electrical and thermal load compensation expense. It can be known that the system operation cost can be reduced and the system operation economy can be improved considering the power support effect of the gas–thermal inertia of the IES.

Comparative Analysis of the Importance of Critical Equipment

The annual total load shedding of each case and the importance assessment indexes of each key equipment are shown in **Table 5**, considering the power support effect of gas–thermal inertia and calculation results of Case 2 to Case 6. The annual total load shedding is 77,049 kW in Case 7.

The importance of different key equipment is related to two aspects. 1) The importance is related to the failure rate of equipment. The higher the failure rate of the equipment, the greater the threat to comprehensive reliability. 2) The importance is related to the critical degree of the equipment. For example, the CHP unit undertakes the power supply and gas supply functions at the same time, and the equipment has a high coupling degree and large power supply. Therefore, when failure occurs, the other equipment is difficult to be provided with power support completely, which has a greater impact on the reliability of the system. As a typical piece of equipment for gas heating, the gas-fired boiler has a low coupling degree and power supply. Therefore, when the gas-fired boiler fails, the synergistic adjustment of the CHP unit, thermal storage, gas inertia, and thermal inertia can buffer its influence on system reliability. The greater the importance assessment index of energy conversion equipment, the greater its impact on system reliability. It is a weak node that should be focused on and protected to reduce system operation risks.

The annual total load shedding of each case and the importance assessment indexes of each key equipment, considering the calculation results of Case 15 to Case 21 without the power support effect of gas–thermal inertia, are as follows. The annual total load shedding is 85,548 kW in Case 21. The results of Case 16 to Case 20 are shown in **Table 6**.

It can be seen from the above results that the order of importance of each key equipment remains unchanged when the failure rate and critical degree of equipment are affected, including/excluding the gas–thermal inertia characteristics. Therefore, the key equipment with a large importance assessment index is indeed the weak node that the system operator should focus on and protect. The difference is that the importance assessment index of each key equipment is larger when the gas–thermal inertia is excluded, as shown in **Figure 7**. The reason is that due to the weak power support ability and poor reliability of the system, even a single failure of key equipment may cause serious load shedding consequences. In conclusion, considering the gas–thermal inertia is beneficial to the long-term reliable and stable operation of the system.

CONCLUSION

This study carries out a reliability assessment of the IES considering the rich flexibility of IES gas–thermal slow dynamic characteristics. The reliability assessment model of the IES is established, the influence of gas–thermal inertia on the reliability assessment of the IES is analyzed, and the importance of different key equipment nodes for the long-term stable and reliable operation of the IES is studied. The results of the case verify the rationality of the proposed model, and the following conclusions can be drawn: 1) when the reliability assessment is carried out considering the gas–thermal inertia of the IES, the size and frequency of load shedding can be reduced, the system operation risk caused by heavy load can be alleviated, and the long-term operation reliability of the system can be improved; 2) considering the power support function of the gas–thermal inertia of the IES, the system operation cost can be reduced and the system operation economy can be improved; and 3) the greater the importance assessment index of energy conversion equipment, the greater its impact on system reliability. Therefore, it is the weak node that should be focused on and protected to reduce system operation risks.

The reliability assessment model of the IES with gas–thermal inertia proposed in this article provides a new idea for the reliability assessment of the IES presently. In the next stage, the model-data hybrid drive method will be used to assess reliability and improve the efficiency of reliability assessment to improve the current model-driven assessment method with a relatively slow calculation speed to be further applied to practical complex systems.

DATA AVAILABILITY STATEMENT

The original contributions presented in the study are included in the article/supplementary material, and further inquiries can be directed to the corresponding author.

AUTHOR CONTRIBUTIONS

All authors contributed to conception and design of the study, organized the database, performed the statistical analysis, wrote the first draft and sections of the manuscript, contributed to manuscript revision, and read and approved the submitted version.

REFERENCES

Antenucci, A., and Sansavini, G. (2018). Gas-constrained Secure Reserve Allocation with Large Renewable Penetration. *IEEE Trans. Sustain. Energy* 9 (2), 685–694. doi:10.1109/tste.2017.2756091

Bansal, M., Khatod, D. K., and Saini, R. P. (2014). "Modeling and Optimization of Integrated Renewable Energy System for a Rural Site[C]," in Proceeding of the 2014 International Conference on Reliability Optimization and Information Technology (ICROIT), Noida, India, February 2014 (IEEE).

Bao, Z., Ye, Y., and Wu, L. (2020). Multi-timescale Coordinated Schedule of Interdependent Electricity-Natural Gas Systems Considering Electricity Grid Steady-State and Gas Network Dynamics[J]. *Electr. Power Energy Syst.* 118 (1), 1–10. doi:10.1016/j.ijepes.2019.105763

Cheng, C., Sun, Q., Huang, Y., and Dong, Q. (2020). "Reliability Evaluation of Integrated Energy System Based on Coupling Equipment Failure[C]," in Proceeding of the Chinese Automation Congress (CAC), Shanghai, China, November 2020 (IEEE).

Clegg, S., and Mancarella, P. (2016). Integrated Electrical and Gas Network Flexibility Assessment in Low-Carbon Multi-Energy Systems. *IEEE Trans. Sustain. Energy* 7 (2), 718–731. doi:10.1109/tste.2015.2497329

Fang, J., Zeng, Q., Ai, X., Chen, Z., and Wen, J. (2018). Dynamic Optimal Energy Flow in the Integrated Natural Gas and Electrical Power Systems [J]. *IEEE Trans. Sustain. Energy* 9 (1), 188–198. doi:10.1109/tste.2017.2717600

Fei, M., Yi, P., Chen, Z., Shi, T., Sha, H., and Zheng, J. (2019). "Research on Multi-Energy Power Flow Calculation of Thermoelectric Coupling Integrated Energy System[C]," in Proceeding of the IEEE Conference on Energy Internet and Energy System Integration (EI2), Changsha, China, November 2019 (IEEE).

Lei, Z., and Yi, L. (2018). Combined Heat and Power Scheduling Utilizing Building-Level Thermal Inertia for Short-Term Thermal Energy Storage in District Heat System[J]. *IEEE Trans. Electr. Electron. Eng.* 13 (1), 804–814. doi:10.1002/tee.22633

Li, X., Li, W., Zhang, R., Jiang, T., Chen, H., and Li, G. (2020). Collaborative Scheduling and Flexibility Assessment of Integrated Electricity and District Heating Systems Utilizing Thermal Inertia of District Heating Network and Aggregated Buildings[J]. *Appl. Energy* 258 (1), 1–20. doi:10.1016/j.apenergy.2019.114021

Li, W., Tang, W., Zheng, J., and Wu, Q. H. (2020). "Reliability Modeling and Assessment for Integrated Energy System: a Review of the Research Status and Future Prospects[C]," in Proceeding of the IEEE Sustainable Power and Energy Conference (iSPEC), Chengdu, China, November 2020 (IEEE).

Liu, F., Bie, Z., and Wang, X. (2019). "Energy and Reserve Co-optimization for Combined Electricity and Natural Gas Market[C]," in Proceeding of the IEEE Power & Energy Society General Meeting, Atlanta, United States, August 2019 (IEEE).

Mu, Y., Chen, W., Yu, X., Jia, H., Hou, K., Wang, C., et al. (2020). A Double-Layer Planning Method for Integrated Community Energy Systems with Varying Energy Conversion Efficiencies[J]. *Appl. Energy* 279 (1), 1–12. doi:10.1016/j.apenergy.2020.115700

Pan, Z., Guo, Q., and Sun, H. (2017). Feasible Region Method Based Integrated Heat and Electricity Dispatch Considering Building Thermal Inertia[J]. *Appl. Energy* 192 (1), 395–407. doi:10.1016/j.apenergy.2016.09.016

Qin, X., Sun, H., Shen, X., Guo, Y., Guo, Q., and Xia, T. (2019). A Generalized Quasi-Dynamic Model for Electric-Heat Coupling Integrated Energy System with Distributed Energy Resources[J]. *Appl. Energy* 251 (1), 1–12. doi:10.1016/j.apenergy.2019.05.073

Saedi, I., Mhanna, S., and Mancarella, P. (2021). Integrated electricity and gas system modelling with hydrogen injections and gas composition tracking. *Applied Energy* 303, 117598. doi:10.1016/j.apenergy.2021.117598

Saldarriaga, C. A., Hincapie, R. A., and Salazar, H. (2013). A Holistic Approach for Planning Natural Gas and Electricity Distribution Networks. *IEEE Trans. Power Syst.* 28 (4), 4052–4063. doi:10.1109/tpwrs.2013.2268859

Valdivia, P., Barraza, R., Saldivia, D., Gacitúa, L., Barrueto, A., and Estay, D. (2020). Assessment of a Compressed Air Energy Storage System Using Gas Pipelines as Storage Devices in Chile. *Renew. Energy* 147, 1251–1265. doi:10.1016/j.renene.2019.09.019

Wang, Q., Tao, S., Du, X., Zhong, C., and Tang, Y. (2019). Coordinated Control Strategy for Multi Micro Energy Systems within Distribution Grid Considering Dynamic Characteristics and Contradictory Interests[J]. *IEEE Access* 7 (1), 139548–139559. doi:10.1109/access.2019.2943926

Wei, N., Lin, L., Yue, X., Junyong, L., Yuan, H., and Pengfei, W. (2020). Reliability Evaluation of Integrated Energy System Based on Markov Process Monte Carlo Method [J]. *Power Syst. Technol.* 44 (1), 150–158. doi:10.13335/j.1000-3673.pst.2019.0047

Wei, H., Zhang, Y., Wang, Y., Hua, W., Jing, R., and Zhou, Y. (2022). Planning Integrated Energy Systems Coupling V2G as a Flexible Storage. *Energy* 239, 122215. doi:10.1016/j.energy.2021.122215

Wu, D., Han, Z., Liu, Z., Li, P., Ma, F., Zhang, H., et al. (2021). Comparative Study of Optimization Method and Optimal Operation Strategy for Multi-Scenario Integrated Energy System. *Energy* 217, 119311. doi:10.1016/j.energy.2020.119311

Xu, X., Zhou, Y., Qadrdan, M., and Wu, J. (2019). "Unlocking the Flexibility of CHP in District Heating Systems to Provide Frequency Response[C]," in Proceeding of the IEEE Milan PowerTech Conference, Milan, Italy, June 2019 (IEEE).

Conflict of Interest: The authors declare that the research was conducted in the absence of any commercial or financial relationships that could be construed as a potential conflict of interest.

Publisher's Note: All claims expressed in this article are solely those of the authors and do not necessarily represent those of their affiliated organizations or those of the publisher, the editors, and the reviewers. Any product that may be evaluated in this article or claim that may be made by its manufacturer is not guaranteed or endorsed by the publisher.